TABLE I

Diode #	1	2	3	4	5	6	7
	ceramic	ceramic	ceramic	ceramic	quartz	quartz	quartz
A/cm^2 x 10^{-4}	1.4	1.9	2.4	2.7	2.4	2.4	2.4
C_p* /pF	0.22	0.22	0.22	0.22	0.08	0.28	0.2
L_p** /pH	30	30	30	30	30	20	45
P/W	6	7.5	8.9	6.5	3.8	8.1	10.2

*C_P is measured by a Boonton RF admittance bridge.
**L_p is evaluated from inductance values published by Kramer [1] and Chang and Ebert [13].

very low negative diode resistance favors diode internal and circuit losses.

If, instead of the ceramic ring (diodes #1–4), a quartz ring with nearly the same dimension (diode #5) is used, the capacitance C_p reduces from 0.22 pF to 0.08 pF and the inductance remains constant. The maximum output power of this type of encapsulated diode, however, is only 3.8 W, though the diode is the same as diode #3 and a low-loss quartz ring is applied. In the case of the used resonator, this behavior can be explained with the aid of Figs. 3 and 5. The resonator is optimized to match a low negative real part with capacitive reactance (see Fig. 3; $l_c = 0.15$ mm). The ceramic ring in addition with the cross-wise bonded gold stripes of diodes #1–4 leads to a transformation with this capacitance character (see Fig. 5, lower half of the Smith Chart), and good matching of the transformed diode and the resonator is possible. The quartz ring, however, with the same bonding lead inductance causes a transformation with inductive character where an optimum matching of the resonator cannot be obtained and only 3.8-W output power can be achieved. Referring to the data of diode #6, a larger value of the capacitance C_p (0.28 pF) in addition with a relatively low inductance L_p (20 pH) leads to a transformation with again capacitive behavior and correspondingly higher output power of 8.1 W can be obtained. A further increase in output power for the same diodes is achievable if the value of the inductance L_p is further increased (to 45 pH for diode #7), and in this case a maximum output power of more than 10 W at 5-percent efficiency was obtained. These results reflect that, depending on the resonator properties, even relatively large parasitics allow an optimum matching if the resonator and the diode transforming network are well designed.

VI. Conclusion

The fabrication of pulsed single-drift IMPATT diodes for millimeter-wave frequencies with different mounting techniques has been described. An inductive-post resonator with reduced waveguide height enables an efficient matching so that more than 10-W peak output power at 5-percent efficiency can be achieved, demonstrating that the single-drift diode can compete with double-drift devices at *V*-band frequencies. The knowledge of the resonator and diode impedance allows a prediction of the needed parasitic reactances which transform the diode impedance for optimum matching. In contrast to the often-stated demand of minimum parasitics, the results show that a relatively large and not a minimum value for the inductance of the connecting lead delivers maximum output power.

Acknowledgment

The authors are very indebted to Dr. A.G. Williamson for sending some of his "School of Engineering Reports." They wish to acknowledge Prof. W. Harth for helpful discussions.

References

[1] N. B. Kramer, "Millimeter-wave semiconductor devices," *IEEE Trans. Microwave Theory Tech.*, vol. MTT-24, pp. 685–693, 1976.
[2] R. J. Wagner, W. W. Gray, and P. V. Cooper, "*X*-band IMPATT microstrip power sources," *IEEE J. Solid-State Circuits*, vol. SC-3, pp. 221–225, 1968.
[3] K. P Weller, R. S. Ying, and D. K. Lee, "Pumps and local oscillators," Air Force Avionics Lab., Tech. Rep. AFAL-TR-75-177, Sept. 1975.
[4] H. J. Kuno and D. L. English, "Nonlinear and large-signal characteristics of millimeter-wave IMPATT amplifiers," *IEEE Trans. Microwave Theory Tech.*, vol. MTT-21, pp. 703–706, 1973.
[5] T. A. Midford and R. L. Bernick, "Millimeter-wave CW IMPATT diodes and oscillators," *IEEE Trans. Microwave Theory Tech.*, vol. MTT-27, pp. 483–492, 1979.
[6] A. R. Kerr, "Low-noise room-temperature and cryogenic mixers for 80–120 GHz," *IEEE Trans. Microwave Theory Tech.*, vol. MTT-23, pp. 781–787, Oct. 1975.
[7] R. Pierzina, to be published.
[8] A. G. Williamson, "Analysis and modeling of two-gap coaxial line rectangular waveguide junctions," *IEEE Trans. Microwave Theory Tech.*, vol MTT-31, pp. 295–302, 1980.
[9] D. Leistner, "Herstellung und Untersuchung von Lawinenlaufzeitdioden und Oszillatoren für *V*- and *W*-Band-Frequenzen," Diss. Techn. Univ. München, 1983.
[10] J. Wenger, "140 GHz 70 mW CW output power with n-type silicon single-drift IMPATT diodes," *Electron. Lett*, vol. 19, pp. 908–909, 1983.
[11] H. G. Unger and W Harth, *Hochfrequenz-Halbleiterelektronik*. Stuttgart: S. Hirzel Verlag, 1972.
[12] W. Harth and M. Claassen, *Aktive Mikrowellendioden*. Berlin: Springer-Verlag, 1981.
[13] S. O'Hara and J. R. Grierson, "A study of the power handling ability of gallium arsenide and silicon, single and double drift impatt diodes," *Solid-State Electron*, vol. 17, pp. 137–153, 1974.
[14] K. Chang and R. L. Ebert, "*W*-band power combiner design," *IEEE Trans. Microwave Theory Tech.*, vol. MTT-28, pp. 295–305, 1980.

X-Band Low-Noise GaAs Monolithic Frequency Converter

K. HONJO, Y. HOSONO, AND T. SUGIURA

***Abstract*—An *X*-band, low-noise GaAs monolithic frequency converter has been developed. Multicircuit functions, such as amplification, filtering, and mixing, were integrated on to a single GaAs frequency converter chip. The frequency converter consists of an *X*-band three-stage low-noise amplifier, an image rejection filter, an *X*-band dual-gate FET mixer, and an IF-band buffer amplifier. To minimize circuit size without degrading performances, an *RC*-coupled buffer amplifier was connected directly after a dual-gate FET mixer IF port, and one-section parallel and series microstrip lines were adopted for the amplifier. One-half-micron (1/2 μm) single-gate FET's and a one-micron (1 μm) dual-gate FET, which have an ion-implanted closely-spaced electrode structure, were used. Either via hole grounds or bonding wire grounds are selectable for the frequency converter. Chip size is 3.4×1.5 mm. The frequency converter provides less than 3-dB noise figure and more than 34-dB conversion gain.**

Manuscript received December 18, 1984; revised July 2, 1985.

K. Honjo is with the Microelectronics Research Laboratories, NEC Corporation, 1-1 Miyazaki, 4-chome, Miyamae-ku, Kawasaki, Kanagawa 213, Japan.
Y. Hosono is with the NEC Corporation, Second LSI Division, Kawasaki, Kanagawa 213, Japan.
T. Sugiura is with the NEC corporation, Space Laser Communication Division, Kawasaki, Kanagawa, Japan.

0018-9480/85/1100-1231$01.00 ©1985 IEEE

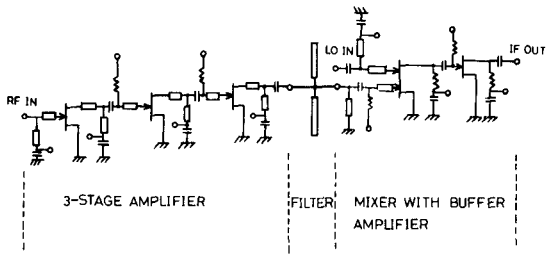

Fig. 1. An equivalent circuit for the X-band low-noise GaAs monolithic-frequency converter.

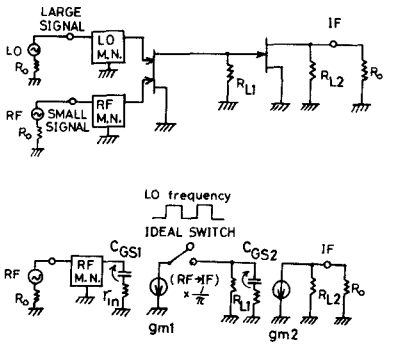

Fig. 2. Approximate operation model for the dual-gate FET mixer with buffer amplifier.

I. Introduction

Low-noise frequency converters are key devices in microwave systems, such as direct broadcast satellite (DBS), radar, and communications. Especially for the DBS application, mass production with low cost and sufficient performance is required for the frequency converters. The frequency converter generally consists of a 12-GHz band low-noise amplifier, an image rejection filter, and a local oscillator. In the present case, the RF signal (11.7–12.2 GHz) is converted to an IF signal (0.9–1.4 GHz) using a local oscillator signal (10.8 GHz). The image-frequency band to be suppressed is 9.4–9.9 GHz. To achieve the requirement, much effort has been made toward the development of GaAs monolithic microwave integrated-circuit (MMIC) technology [1]–[4]. However, most GaAs MMIC's previously reported have a single-circuit function, such as amplification, mixing, filtering, and oscillation, etc. Therefore, low-noise frequency converters were fabricated using several different MMIC chips [1]–[4].

In order to achieve lower cost, an integration of multicircuit functions is considered to be necessary. P. Harrop *et al.* reported the first 12-GHz GaAs monolithic receiver front end [5]. However, this chip (1 cm×1 cm) was too large to achieve mass production. In addition, the performance (noise figure: 4.5 dB, conversion gain: 15 dB) was not sufficient for DBS application. To apply multifunction integrated MMIC's in real systems, the circuit size for each function must be reduced without degrading the performance.

This paper describes considerations and measured performance of a newly developed X-band low-noise GaAs monolithic frequency converter. The frequency converter consists of an X-band low-noise amplifier, an image rejection filter, an X-band dual-gate FET mixer, and an IF-band buffer amplifier. All circuit functions have been fabricated onto a single GaAs chip. The developed frequency converter provides less than 3.0-dB noise figure and more than 34-dB conversion gain.

II. Circuit Design

Fig. 1 shows an equivalent circuit for the X-band low-noise GaAs monolithic frequency converter. The frequency converter consists of an X-band three-stage low-noise amplifier, an image-rejection filter, a dual-gate FET mixer, and an IF-band buffer amplifier.

A. Low-Noise Amplifier

The amplifier has a three-stage configuration. For amplifier circuit design, element values in an FET equivalent circuit were derived by using measured S parameters for a discrete FET. Based on these values, amplifier parameters were optimized by a CAD program. Calculated gain for the amplifier is more than 28 dB over the frequency range from 11.4 to 12.7 GHz. To reduce the chip size, interstage matching networks directly transform FET output impedances into the complex conjugate of the FET input impedances, without transforming them into 50 Ω. For each matching section, one-section parallel and series microstrip lines are used. These lines can also be utilized as dc-bias feed lines. The first stage gate bias voltage and all drain bias voltages are supplied through the lines. Gate bias voltages for the second-stage and the third-stage are supplied through resistors. The resistance is about 10 kΩ. Totally, six bias voltage supplies are required for the amplifier. To obtain the best performance, each bias voltage should be supplied individually. On the other hand, for simplification, a combination of bias supplies is necessary. However, a combination of the drain bias supplies usually causes parasitic oscillations. Therefore, in amplifier measurements, drain bias voltages are supplied individually, while all gate bias voltage supplies are combined.

B. Mixer with Buffer Amplifier

A dual-gate FET was adopted as a mixing device, since filtering circuits can be greatly simplified due to its built-in isolation effect among electrodes. To obtain chip-size reduction and broad-band characteristics, the buffer amplifier has been connected directly after the mixer IF port without employing the IF matching circuit [1]. The buffer amplifier is a one-stage resistor capacitor coupled amplifier.

To predict conversion gain for the dual-gate FET mixer with the buffer amplifier, mixer operation is simplified, as shown in Fig. 2. In this mixer, an RF signal (small signal) is applied to the first gate and a local oscillator (LO) signal (large signal) is applied to the second gate. Then, if we assume that the FET drain current $Ide^{j\omega_{RF}t}$ is ideally switched with 50-percent duty cycle by the local oscillator signal, the Fourier component for $\omega_{RF\text{-}LO}$ becomes

$$\frac{Id}{\pi} e^{j(\omega_{RF}-\omega_{LO})t} \tag{1}$$

where RF and LO are angular frequencies for RF and LO, respectively. In the case of a single-gate FET mixer, the maximum value of conversion transconductance is approximately one third ($\simeq 1/\pi$) of the maximum value of g_m [6]. In Fig. 2, if a lossless RF matching network is assumed, conversion power gain $Gc(\omega_{RF})$ is approximately calculated as

$$Gc(\omega_{RF}) \simeq \frac{(g_{m1}g_{m2}R_{L1}R_{L2})^2 R_0}{\pi^2 C_{GS1}^2 r_{in}(R_{L2}+R_0)^2 \omega_{RF}^2 \{1+(\omega_{RF}-\omega_{LO})^2 C_{SG2}^2 R_{L1}^2\}}. \tag{2}$$

Since mixing devices are nonlinear devices, there are many frequency components to be considered, such as image frequencies and harmonic frequencies. However, to estimate conversion gain characteristics for a dual-gate FET mixer with a buffer amplifier, this approximation can be used.

To determine the RF and LO matching network parameters, a CAD program was used, where the dual-gate FET was treated as two single-gate FET's. In the program, the whole mixer circuit was represented as a two-port network, regarding the RF input port and the local oscillator signal input port as the two ports, where an output port for the buffer amplifier was terminated. The objective is to achieve VSWR reduction at both input and output ports.

Bias voltages for the mixer with the buffer amplifier are supplied through resistors, except for the second gate of the dual-gate FET, as shown in Fig. 1.

C. Filter

The image-rejection filter consists of two $\lambda/4$ open stubs. The stub lengths are slightly different, to achieve broad-band characteristics using the double-tuning effect. From preliminary experiments, about 15-dB rejection was estimated. In addition, the calculation result for the amplifier shows more than 15-dB off-band gain reduction in the image-frequency band. Therefore, totally, 30-dB image rejection is expected for the frequency converter. In a real system, a waveguide is used between a reception antenna and the frequency converter. Since a waveguide is originally a high-pass filter, if a cutoff frequency for the waveguide is chosen between the local oscillator frequency and the lower band edge of the RF signal, realization of more than 70-dB image rejection is not so difficult.

III. Fabrication Process

Fig. 3 shows a perspective view of the basic structure for the frequency converter. The starting material is a Cr-doped HB GaAs substrate. Active layers for FET's and resistive layers for gate bias voltage supplies were formed by selective $^{29}Si^{+}$ implantation, where a dose $D = 3.0\times10^{12}$ cm^{-2} at energy $E = 50$ KeV. Resistive layers for load resistors were formed by selective double implantation of $^{28}Si^{+}$. Conditions for the implantation are $D = 3.0\times10^{13}$ cm^{-2}, $E = 130$ KeV, and $D = 3\times10^{13}$ cm^{-2}, $E = 60$ KeV. The substrates were then capped with CVD-SiO_2 films and annealed at 800°C for 20 min in an H_2 ambient. A dual-gate FET, as well as single-gate FET's, has a closely-spaced electrode structure [7], [8]. Both the gate-to-drain spacing and the gate-to-source spacing are 0.5 μm. The gate metal is self-aligned aluminum. Gold-germanium-nickel was used to form ohmic contacts.

The gate length is 0.5 μm, except for the mixer with a buffer amplifier (1.0 μm). Fig. 4 shows photographs of a single-gate FET for the X-band amplifier and a dual-gate FET for the mixer. Both FET's have four gate fingers. The gate width for the single-gate FET is 280 μm and that for the dual-gate FET is 320 μm. Observed g_{m0}, V_T, and I_{dss} values for the 0.5-μm single-gate FET were 160 ms/mm, -1.4 V, and 200 mA/mm, respectively. Sheet resistivity for the double ion-implanted layers was 180 $\Omega/\square$.

Capacitors are MIM-type, where dielectric material is 2000-Å-thick CVD-SiO_2. The transmission lines, bonding pads, capacitor top plates, as well as fingers for the FET drain and the source, are Au plated. Thickness is 2.5 μm. In the converter chip, either bonding wire grounds or chemically etched via hole grounds can be utilized, since the pads to be grounded are located near the chip periphery.

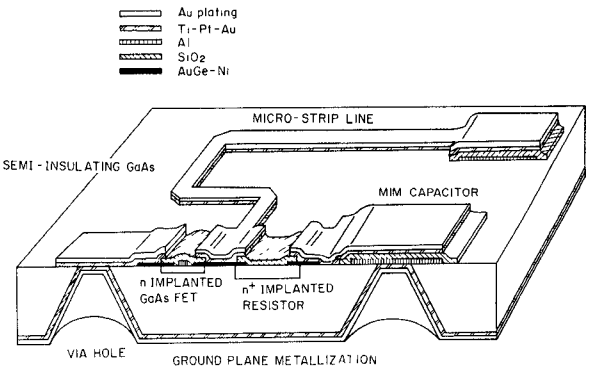

Fig. 3. Perspective view of the frequency converter basic structure.

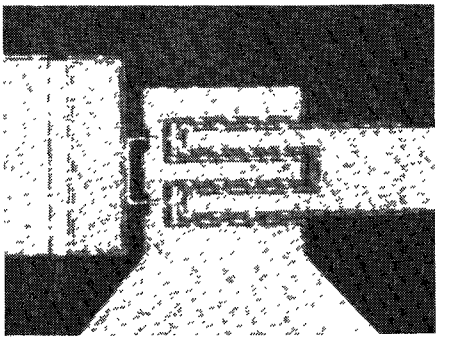

(a)

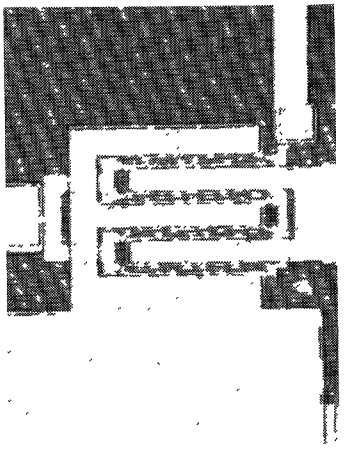

(b)

Fig. 4. Photographs of (a) single-gate FET for X-band amplifier and (b) dual-gate FET for mixer.

Fig. 5 shows photographs of the top and the bottom views of the converter chip. In the figure, via hole A corresponds to pad A'. Chip size is 3.4 mm$\times$1.5 mm. Wafer thickness is 150 μm. For an individual performance check, using the dicing saw, the converter chip can be divided into three components, X-band amplifier, the image rejection filter, and the mixer with buffer amplifier.

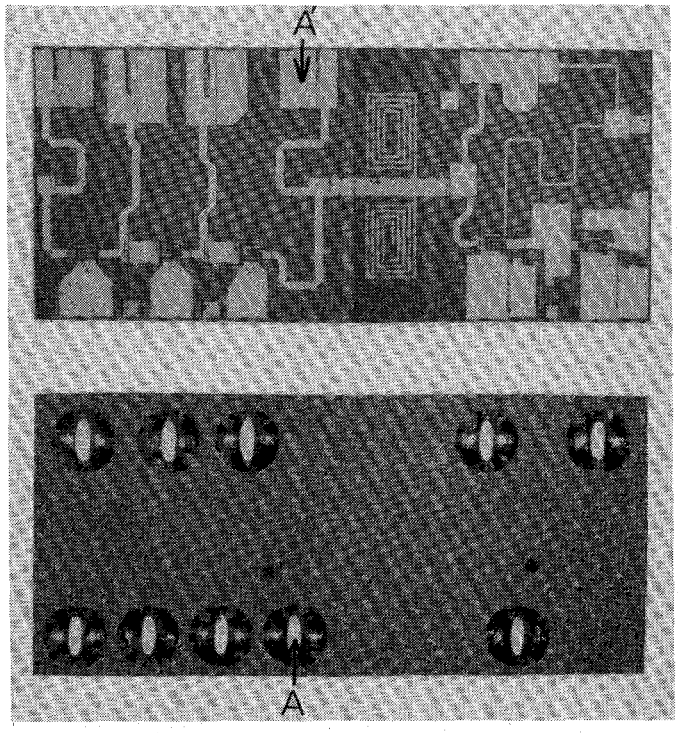

Fig. 5. Top and bottom views of frequency converter chip.

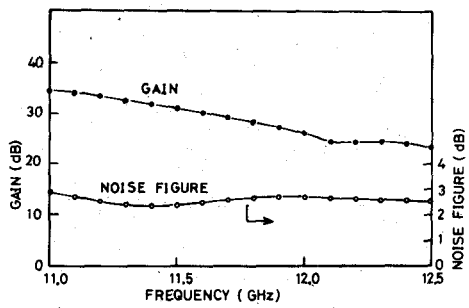

Fig. 6. Measured gain and noise figure characteristics of the GaAs monolithic amplifier.

The microstrip lines in the chip were folded in order to reduce the chip size. However, to avoid parasitic couplings, the spacing between adjacent lines was designed to be as large as possible.

IV. Microwave Performance

The amplifier chip, the mixer chip, and the filter chip, as well as the converter chip, were mounted on chip carriers and tested with bonding wire grounds in a 50-Ω system.

Fig. 6 shows gain and noise figure characteristics for the amplifier. The amplifier has more than 24-dB gain and less than 2.7-dB noise figure for the 11.2–12.4-GHz frequency range. Minimum noise figure is 2.35 dB with 32 dB gain at 11.4 GHz. Input VSWR was less than 1.6, and the output VSWR was less than 1.8 over the 11.2–12.4-GHz range. Saturation power output was 13 dBm. The measured amplifier-frequency band is lower than the designed band by about 1 GHz. This is due to the bonding wire grounds, which are attended with parasitic elements caused by the pads. In case of the bonding wire grounds, since the pads operate as parasitic transmission lines, microstrip line lengths for matching circuits become longer than the designed values. Therefore, the frequency band for the bonding wire

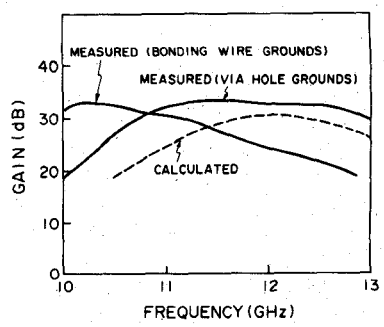

Fig. 7. Measured gain-frequency characteristics comparison between the bonding wire grounded amplifier and the via hole grounded amplifier. Calculated gain is also plotted.

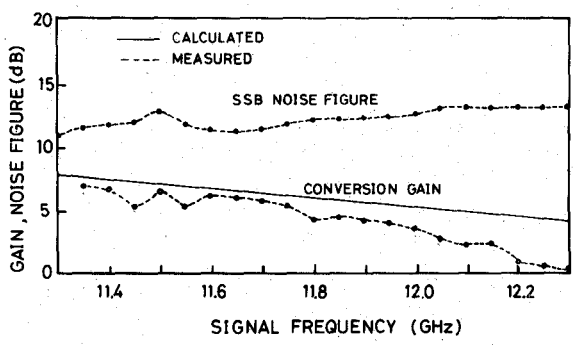

Fig. 8. Measured conversion gain and SSB noise figure of the GaAs monolithic dual-gate FET mixer with buffer amplifier. Calculated conversion gain is also represented.

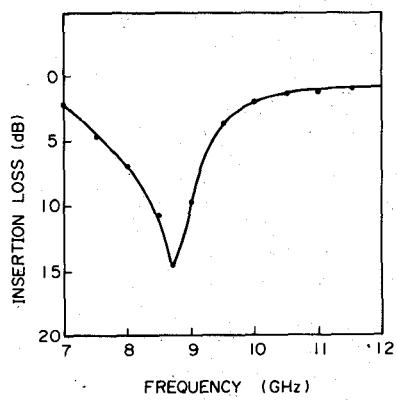

Fig. 9. Insertion loss of the image-rejection filter.

grounded amplifier is shifted to a lower frequency. Fig. 7 shows a comparison between the bonding wire grounded amplifier and the via hole grounded amplifier. The designed value is also shown in the figure. The measured gain for the via hole grounded amplifier, which is close to the designed value, is more than 31 dB over 11.7–12.7 GHz. This measured gain is higher than the designed value by about 2 dB. This is due to the S parameters used for the calculation. The S parameters were obtained from a discrete FET having a transconductance of 130 mS/mm. However, FET transconductance in the converter chip is improved to 160 mS/mm.

Fig. 8 shows the measured conversion gain and SSB noise figure for the mixer with buffer amplifier. The local oscillator frequency is 10.8 GHz and its power level is 8 dBm. The mixer has more than 1-dB conversion gain and less than 13-dB SSB

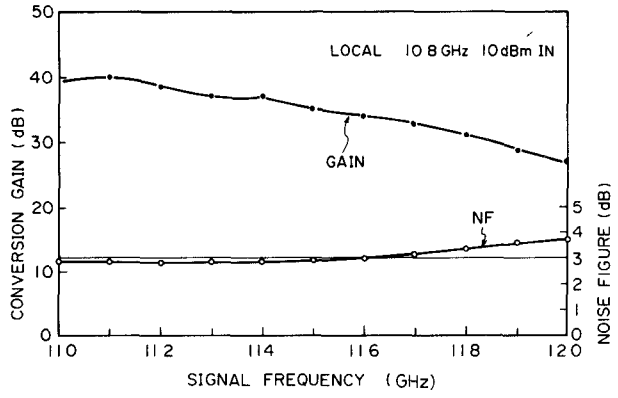

Fig. 10. Measured conversion gain and noise figure of the GaAs fully-monolithic frequency converter.

noise figure from the 11.3–12.2-GHz range. The figure also shows calculated conversion gain, which is in comparatively good agreement with the measured results. VSWR at the mixer RF input port was measured, supplying 8-dBm local oscillator power to the local oscillator signal input port. The VSWR was less than 3 over the 11.3–12.2-GHz range. The VSWR didn't depend strongly on the local oscillator power level.

Insertion loss for the filter is shown in Fig. 9. Maximum insertion loss is 15-dB at 8.7 GHz. Measured center frequency for the image rejection is lower than the designed frequency (9.65 GHz). Insertion loss for the RF band is approximately 1 dB. Measured relative bandwidth for more than 10-dB insertion loss for the double-tuning filter was about 40-percent superior to that for the single-tuning filter. Measured VSWR in the RF signal band was less than 2.5.

Since VSWR values for the amplifier, the filter, and the mixer is less than 3, appropriate total performances for the frequency converter chip can be expected.

Fig. 10 shows the experimental results for total conversion gain and noise figure on the GaAs fully-monolithic frequency converter. As shown in the figure, the frequency converter provides more than 34-dB conversion gain and less than 3.0-dB noise figure from 11.0–11.6 GHz. Saturation power output for the frequency converter was 7 dBm. DC power dissipation was 225 mW.

Since the frequency band and noise figure for the frequency converter are mainly determined by the amplifier characteristics, the frequency band for the frequency converter can be modified, mainly by changing the amplifier band.

V. Conclusion

Design considerations and microwave performances for the newly developed *X*-band GaAs monolithic frequency converter have been described. Multicircuit functions such as amplification, filtering, and mixing were integrated onto a single GaAs chip. The frequency converter provided more than 34-dB conversion gain and less than 3-dB noise figure in the 11.0–11.6-GHz range.

It has been demonstrated that reasonable performance can be obtained from a one-chip construction, MMIC-frequency converter, in which multicircuit functions were integrated. After proper modification based on the results, the frequency converter will be used in *X*-band systems, such as direct broadcast satellite reception, radar, or microwave communication systems.

Acknowledgment

The authors would like to thank T. Ozawa for ion implantation. They also would like to thank Y. Takayama and K. Kohzu for their constant encouragement throughout this work.

References

[1] T. Sugiura, H. Itoh, T. Tsuji, and K. Honjo, "12-GHz-band low-noise GaAs monolithic amplifiers" *IEEE Trans. Microwave Theory Tech.*, Vol. MTT-31, pp. 1083–1088, Dec. 1983.

[2] T. Sugiura, K. Honjo, and T. Tsuji, "12 GHz-band GaAs dual-gate MESFET monolithic mixer," in *1983 IEEE GaAs IC Symp Dig.*, Oct. 1983, pp. 3–6.

[3] C. Kermarrec, P. Harrop, C. Tsironis, and J. Faguet, "Monolithic circuits for 12 GHz direct broadcasting satellite reception," in *Microwave and Millimeter Wave Monolithic Circuit Symp. Dig.*, June 1982, pp. 5–10.

[4] S. Hori, K. Kamei, K. Shibata, M. Tatematsu, K. Mishima, and S. Okano, "GaAs monolithic MIC's for direct broadcast satellite receivers," *IEEE Trans. Microwave Theory Tech.*, vol. MTT-31, pp. 1083–1088, Dec. 1983.

[5] P. Harrop, P Lesarte, and A. Collet, "GaAs integrated all-front-end at 12 GHz," in *1980 GaAs IC Symp. Res. Abstracts*, paper no. 28.

[6] R A. Pucel, D. Masse, and R. Bera, "Performance of GaAs MESFET mixers at *X*-band," *IEEE Trans. Microwave Theory Tech.*, vol. MTT-24, pp. 351–360, June 1976.

[7] K Honjo, T Sugiura, T Tsuji, and T. Ozawa, "Low-noise low-power-dissipation GaAs monolithic broad-band amplifiers," *IEEE Trans. Microwave Theory Tech.*, vol. MTT-31, pp 412–417, May 1983.

[8] T Furutsuka, T. Tsuji, F. Katano, A. Higashisaka, and K Kurumada, "Ion-implanted E/D type GaAs IC technology," *Electron. Lett.*, vol. 17, no. 25/26, pp. 944–945, Dec. 1981.

A Novel Rectangular Waveguide with Double T-Septums

GOPA GUHA MAZUMDER AND PRADIP KUMAR SAHA

***Abstract*—A new rectangular waveguide with two T-shaped septums in place of solid rectangular ridges has been analyzed theoretically by the Ritz–Galerkin technique and is found to have superior cutoff and bandwidth characteristics of the dominant TE_{10} mode compared to the conventional ridged guides. Numerical data are presented and compared with those of symmetric double-ridged guides with identical gap parameters.**

I. Introduction

The ridges in rectangular waveguides are well known for their ability to increase both the cutoff wavelength and bandwidth of the dominant mode [1],[2]. The ridge dimensions can be optimized separately for the cutoff and bandwidth. Further improvements in these features are possible with dielectric filling of the ridge gap [3].

We propose a novel rectangular waveguide structure that is capable of significant improvement over the conventional ridged waveguide in respect of the cutoff wavelength and bandwidth of the dominant mode, even without any dielectric loading. The ridges are now made T-shaped instead of solid rectangular blocks as shown in Fig. 1. The structure remains homogeneous and should be much lighter as well.

Determination of the complete eigenvalue spectrum is not our aim at this time. It is known that for typical values of about 0.5 of the waveguide aspect ratio b/a, the dominant and the first higher order modes are TE_{10} and TE_{20}, respectively, in a conven-

Manuscript received January 10, 1985; revised June 24, 1985

The authors are with the Institute of Radio Physics and Electronics, 92 Acharya Prafulla Chandra Rd., Calcutta-700009, India.

0018-9480/85/1100-1235$01.00 ©1985 IEEE